Isolation Improvement of Two Tightly Coupled Antennas Operating in Adjacent Frequency Bands Using Filtering Structures

JIAYIN GUO[1] (Graduate Student Member, IEEE), FENG LIU [1] (Graduate Student Member, IEEE), LUYU ZHAO [1] (Senior Member, IEEE), GUAN-LONG HUANG [2] (Senior Member, IEEE), YINGSONG LI [3] (Senior Member, IEEE), AND YINGZENG YIN[1] (Member, IEEE)

[1]National Key Laboratory of Antennas and Microwave Technology, Xidian University, Xi'an 710071, China

[2]College of Electronics and Information Engineering, Shenzhen University, Shenzhen 518060, China

[3]College of Information and Communication Engineering, Harbin Engineering University, Harbin 150001, China

CORRESPONDING AUTHOR: L. ZHAO (e-mail: lyzhao@xidian.edu.cn)

ABSTRACT In this paper, a mutual coupling reduction technique using filtering structures between two antennas resonating in adjacent frequency bands is proposed. Two patch antennas resonating at low band (4.8-5.0 GHz, part of 5G Band N79) and high band (5.15-5.35 GHz, part of IEEE 802.11 ax 5 GHz Band), which are close to each other in frequency spectrum, are used as an illustrative example. The decoupling structure consists of two open-loop resonators with filtering function coupled to the feed line on its edges. By loading the filtering structures, the isolation between the two antennas is improved from poorer than 15 dB to more than 25 dB when the reflection coefficients are still satisfactory in their respective operating frequency bands, showing significant improvements compared to the reference antennas where no filtering structures are introduced. The proposed method can be easily applied to either mobile terminal or 5G CPE (Customer Premise Equipment) devices where both 5G and Wi-Fi are installed as well as many other antennas with similar application scenarios.

INDEX TERMS Adjacent frequency bands, filtering structures, mutual coupling reduction, patch antenna, Wi-Fi, 5G.

I. INTRODUCTION

IT IS in the era where wireless communication has become indispensable and evolving dramatically. The commercialization of the 5th generation (5G) wireless systems [1], followed by the 6th generation Wi-Fi communication systems [2], making the existing scarce frequencies even more crowded. Currently, the 5G frequency bands N7 and N41 are adjacent to the Wi-Fi 2.4 GHz band. Meanwhile, the 5G frequency bands N77∼N79 are also in close proximity to the Wi-Fi 5 GHz band, as shown in Fig. 1, not to mention the coexisting LTE bands which will still be in operation for a long time.

To ensure an antenna operating with desired performance in a multiple-antenna environment, the spacing between the antennas is usually kept above $\lambda_0/2$ (λ_0 represents the free-space wavelength at center frequency). This is true not only for MIMO antennas who are transmitting and receiving signal in the very same frequency channels, but also for antennas whose working frequencies are adjacent. As a matter of fact, it might be more crucial for antennas resonating in adjacent frequency bands to be well isolated since they commonly belong to different communication systems where no coordinating mechanisms exist. In other words, it is highly possible that one antenna is transmitting while the other one is in its receiving mode. It is well understood that transmitting power level for most wireless communication systems must be much higher than the sensitivity of a nearby receiver. Therefore, the mutual coupling between
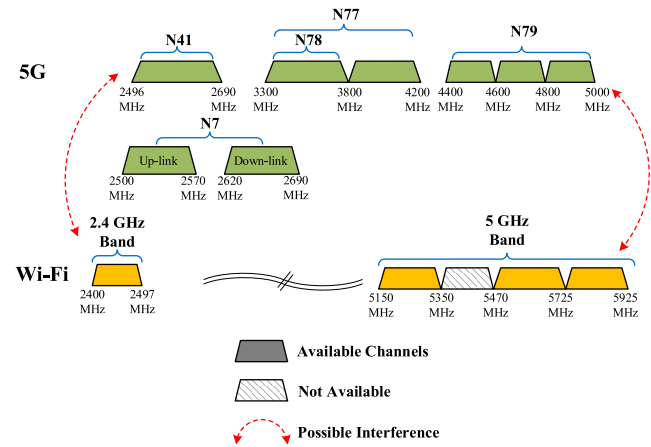
FIGURE 1. Frequency bands for 5G and Wi-Fi where possible interferences may occur.
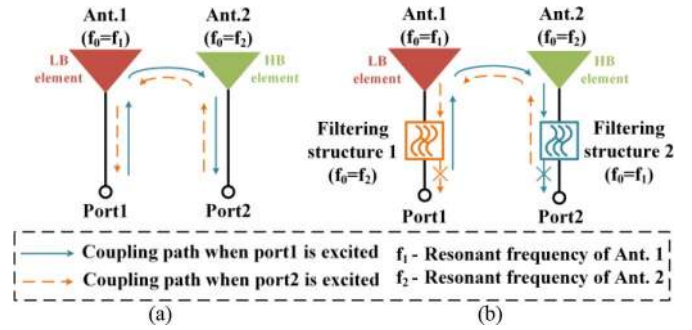

FIGURE 2. Diagram of the coupling mechanism between two antennas resonating in adjacent frequency bands: (a) without filtering structure; and (b) with filtering structure.

antennas in adjacent frequency bands must be taken into consideration [3]–[5].

There are plenty of published papers working on mutual coupling reduction for single band [6]–[17] and dual-band [18]–[22] MIMO antennas where antennas are resonating in the very same frequency bands. Among these designs, most antennas to be decoupled are identical to each other. Currently, there are not many works concerning antennas operating in adjacent frequency bands. For antennas resonating in nearby spectrum, filtering structures have been applied to coupled antennas to improve the port isolation [23], [24]. In [23], the proposed feed network can achieve broadband decoupling with loading high-pass substrate integrated waveguide (SIW) and low-pass spoof surface plasmon polariton (SSPP). In [24], the presented filtering antenna element can improve the port isolation due to its high out-of-band radiation rejection characteristic, in which the radiation of the high band (HB) subarray is suppressed in the low band (LB) and vice versa. Choke radiators are also used to suppress the mutual coupling between low band and high band base station antennas [25]. While in [26], frequency selective surface (FSS) are used to solve the coupling issue whose scenario is similar to that in [25].

In this paper, filtering structures composed of open loop resonators are adopted as part of the feeding line to reduce mutual coupling among patch antennas operating in adjacent bands. The transmission notch can be easily manipulated by adjusting the size of the open-loop resonators at the feeding lines of the low and high band antennas resonating at 4.9 GHz and 5.25 GHz respectively. Results show that introducing these resonators and the transmission notches into the patch antennas operating in adjacent frequency bands is able to improve their isolation significantly.

The rest of the paper is organized in the following manner. The proposed design and the working mechanism of the mutual coupling reduction are elaborated in Section II. To verify the design feasibility of the work, simulated and

measured results will be demonstrated and analyzed in Section III. Conclusion is drawn in Section IV.

II. ANTENNA CONFIGURATION AND ANALYSIS

In this work, the two antennas operating in adjacent bands are studied, as shown in Fig. 2(a). The designed LB and HB antennas are operating at very close frequencies, i.e., 4.9 GHz and 5.25 GHz respectively. In order to minimize the space occupation, the two antennas are placed in close proximity to each other, which will inevitably cause excessive interference between them. The coupling paths between the two antennas is illustrated in Fig. 2. It can be seen from the coupling paths marked in blue in Fig. 2(a) that, when the LB antenna element is excited, a part of electromagnetic (EM) field radiated by the LB element is coupled to the HB element, which would cause an increase in mutual coupling and deterioration in radiation performance. However, when the proposed decoupling structure with filtering function is loaded around the feeding structure of the HB element, the EM field generated by the LB antenna can be absorbed by this structure, which can greatly improve the port isolation at LB and further improve the antenna performance, as depicted in Fig. 2(b). The same analysis process can be applied when the HB antenna is excited. Once the filtering structure is loaded around the feed-line of the LB antenna, the EM waves coupled by the HB antenna can also be effectively suppressed and the port isolation between the two antennas is enhanced. The coupling paths in this case are marked with orange lines in Fig. 2.

A. GEOMETRY OF THE PROPOSED ANTENNA

Based on the above analysis, the proposed antennas resonating in adjacent frequency bands with the filtering structure are shown in Fig. 3, which is arranged along the *y*-axis. It consists of two patches, two feeding networks with filtering structures, and a ground plane. The filtering structures consist of two open-loop resonators coupled to the feed-line on its edges. Both the LB and HB patch antennas are fabricated on the top of the FR4 substrate with a relative permittivity of 4.4 and a thickness of 0.8 mm. And two feeding networks are printed on the top of another substrate with the same
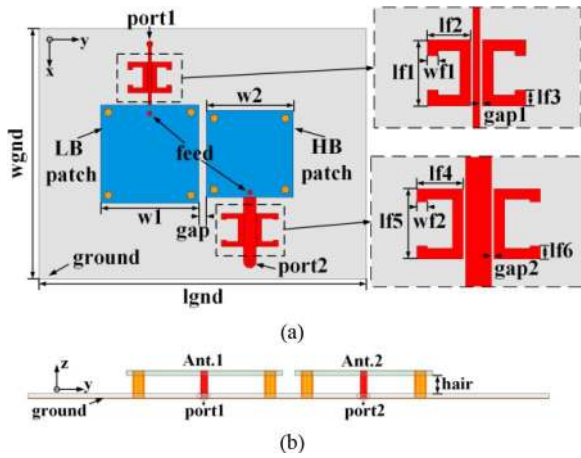
FIGURE 3. Geometry of the proposed antenna. (a) Top view. (b) Side view.

TABLE 1. Optimized parameters of the proposed antenna (unit: mm).

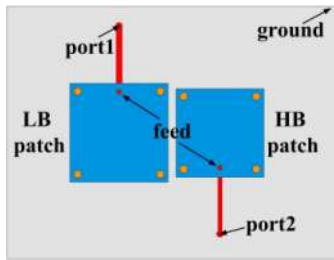| Parameters	lgnd	wgnd	w1	w2	gap	gap1
Value	106	80	25.5	22.5	1	0.1
Parameters	gap2	wf1	wf2	lf1	lf2	lf3
Value	0.1	1.3	1.3	7.9	5.2	1.9
Parameters	lf4	lf5	lf6	hair		
Value	5.7	8.6	1.6	3		

FIGURE 4. Geometry of the reference antenna.

relative permittivity and thickness, whereas the ground plane is printed on the bottom of the substrate. The edge-to-edge spacing between the HB and LB patches is set to 1 mm ($0.016 \lambda_0$ at 4.9 GHz) so as to achieve a compact size. The other parameters of the antennas are listed in Table 1.

In order to better illustrate the effect of the filtering structure on the antennas decoupling, two patch antennas without any additional decoupling structure are shown in Fig. 4 for reference. The comparisons of simulated S-parameters between the reference antennas and the proposed antennas are shown in Fig. 5. It can be observed that $|S_{11}|$ of the reference antennas is less than -10 dB in the LB (4.8-5.0 GHz, part of 5G Band N79) and $|S_{22}|$ is below -10 dB in the HB (5.15-5.35 GHz, part of IEEE 802.11 ax 5GHz Band). As the operating bands of the two antennas are very close (the center frequency of the HB is only 1.07 times of LB), the isolation between the two ports is very poor, which is only about 15 dB at both LB and HB. Under the premise of ensuring that the antennas are well matched, the antennas are able to achieve isolation improvement from 15 dB to
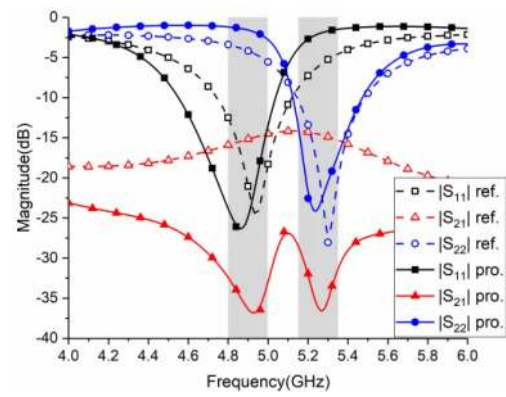

FIGURE 5. Simulated S-parameters of the proposed antenna (with filtering structure) and reference antenna (without filtering structure).
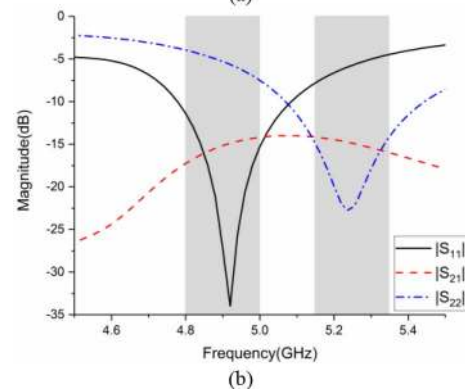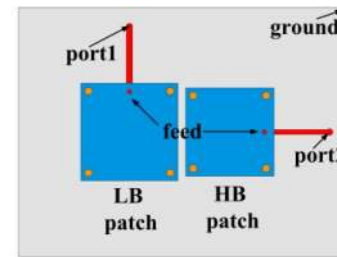

FIGURE 6. (a) Geometry of the antenna with two ports fed orthogonally. (b) The simulated results of S-parameters for this antenna.

about 37 dB at 4.9 GHz and 5.25 GHz with loading the proposed filtering structure, which shows the proposed filtering structures have a very good decoupling effect on the coupled antennas.

Meanwhile, as shown in Fig. 6(a), the antennas working in adjacent frequency bands with two ports fed orthogonally are also simulated and analyzed as another reference antennas. The simulated S-parameters of this antennas are shown in Fig. 6(b). It can be observed that the isolation is also poor (only about 15 dB) in the two operating bands although the antennas are well matched, which implies the method of orthogonal feeding cannot reduce their mutual coupling effectively. Therefore, it is very meaningful using the proposed filtering structures to improve the port
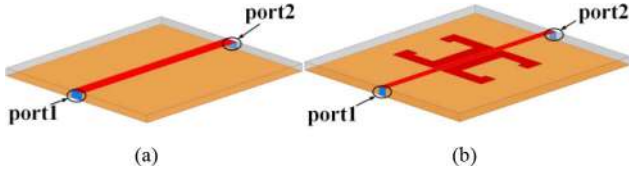
FIGURE 7. Geometry of the microstrip transmission line (a) without filtering structure and (b) with filtering structure.
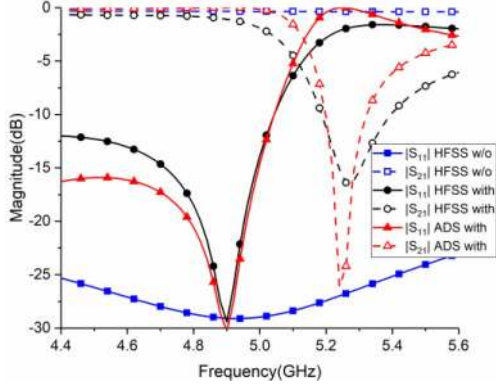

FIGURE 8. The simulated S-parameters of the microstrip transmission line with and without the filtering structure (Case 1).
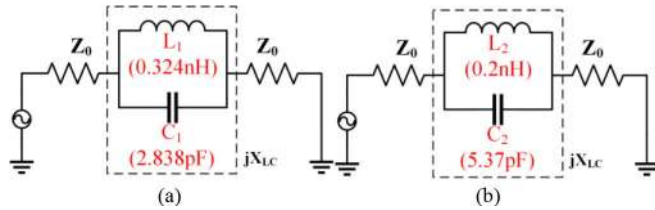

FIGURE 9. The equivalent circuit of the microstrip transmission with the proposed filtering structure. (a) Case 1, (b) Case 2.

isolation of the two antennas operating in adjacent frequency bands.

B. PRINCIPLE OF MUTUAL COUPLING SUPPRESSION

In order to clearly explain the principle of mutual coupling suppression, the feed-line with and without the aforementioned filtering structures is extracted for analysis as depicted in Fig. 7.

Case 1: First of all, the case of microstrip transmission line with resonance at LB (4.9 GHz) and filtering characteristics at HB (5.25 GHz) is investigated. The EM simulation results are shown in Fig. 8. It can be seen that the port isolation at the HB can be effectively improved when the filtering structures with HB coupling suppression is loaded near the feed-line of the LB antenna. Moreover, the microstrip transmission line with the filtering structures exhibits an obvious band-stop characteristic at 5.25 GHz, and the coupling coefficient between the two ports achieves 15 dB reduction at 5.25 GHz while the transmission line is well matched at 4.9 GHz. The total length of the filtering structures is about half wavelength at HB.

Meanwhile, as shown in Fig. 9(a), the filtering structures can be equivalent to a parallel LC resonant circuit, which are connected in series in the main circuit. Therefore, the reactance of the whole LC circuit can be calculated by:

$$X_{LC} = \frac{1}{j}\left(\frac{1}{j\omega C + 1/j\omega L}\right) = \frac{1}{\omega_0^2 C/\omega - \omega C} \qquad (1)$$

where ω_0 represents the resonant angular frequency of the equivalent circuit. When the LC circuit resonates ($\omega = \omega_0$), the impedance of the port tends to infinity, thus preventing current propagation to the feeding port. The value of L and C in the equivalent circuit can be calculated according to the formula in [27]. The equivalent capacitance C is obtained as follows:

$$C = \frac{\omega_c}{Z_0 g_1} \frac{1}{\omega_0^2 - \omega_c^2} \qquad (2)$$

The resonance frequency f_0 of the filtering structures and the 3-dB cut-off frequency f_c of |S_{21}| can be extracted from the frequency response curve in EM simulation, and the corresponding angular frequencies ω_0 and ω_c can be further obtained with the same approach. Finally, the value of capacitance C can be figured out.

According to the resonance condition and the equivalent capacitance C, the equivalent inductance L can be given as follows:

$$L = \frac{1}{\omega_0^2 C} = \frac{1}{4\pi^2 f_0^2 C} \qquad (3)$$

From the above analysis, the component parameters of the equivalent circuit of Case 1 can be calculated, and L = 0.324 nH and C = 2.838 pF are obtained after a fine-tuning process. The numerical results of the equivalent circuit by commercial circuit simulator ADS are also depicted in Fig. 8. The results show that the frequency characteristic curve of EM simulation is in good agreement with that of the circuit simulation, which demonstrates the feasibility of the LC equivalent circuit model.

Case 2: The microstrip transmission line with resonance at HB (5.25 GHz) and filtering characteristics at LB (4.9 GHz) can also be analyzed using the principle of equivalent circuits. In this case, the total length of the filtering structures is about half wavelength at LB. As can be seen from the EM simulated results in Fig. 10, after loading the proposed filtering structures, the coupling coefficient at LB can be significantly reduced. Meanwhile, the capacitance C and the inductance L in the equivalent circuit of Case 2 can be obtained according to the above deduced formulas. As shown in Fig. 9(b), L = 0.2 nH and C = 5.37 pF can be finalized after a fine-tuning under this case. And a good agreement between EM and circuit simulated results can be observed from Fig. 10. Through the analysis of these two cases, the transmission zeros at both bands shown in Fig. 5 have been well validated.

The comparison of vector current distribution with and without the filtering structures is plotted in Fig. 11. From
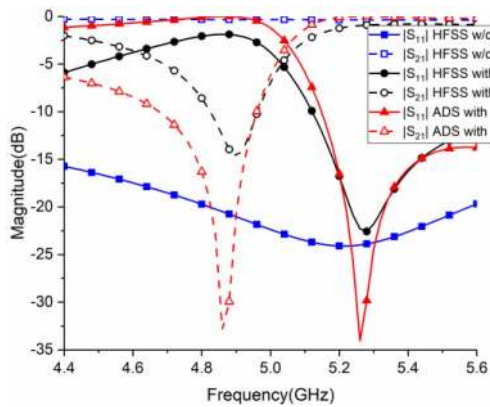
FIGURE 10. The simulated S-parameters of the microstrip transmission line with and without the filtering structure (Case 2).
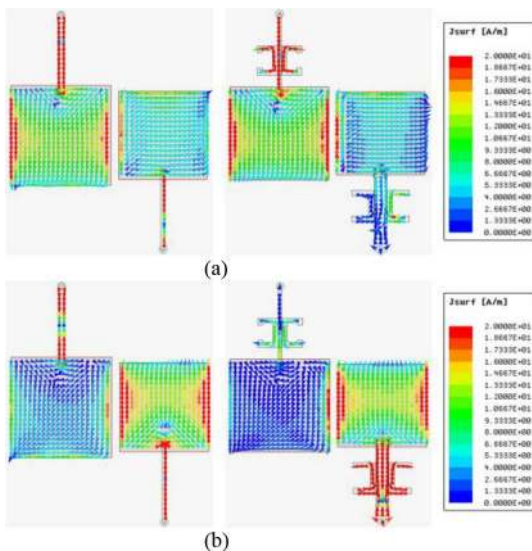

FIGURE 11. Current distributions on the patch and feed line (a) when LB antenna is excited at 4.9 GHz, (b) when HB antenna is excited at 5.25 GHz.

Fig. 11(a), when the LB antenna is excited, a strong current distribution can be observed on the feed-line of the HB antenna at 4.9 GHz under the condition without the filtering structures. After loading the proposed structures, the current distributed on the feed-line of the HB antenna is suppressed obviously, which means an effective isolation improvement is achieved at the lower operating band. A similar phenomenon can also be seen from Fig. 11(b), when HB antenna is excited, the current distributed on the feed-line of the LB antenna is also suppressed at 5.25 GHz after loading the proposed filtering structures. Thus, the port isolation between the LB and HB elements is improved at both working bands.

From the above analysis, it can be concluded that the frequency band of decoupling can be controlled by adjusting the length of the proposed filtering structures. Therefore, the effects of two key parameters, i.e., *lf2* and *lf4*, on the antennas decoupling are analyzed separately.
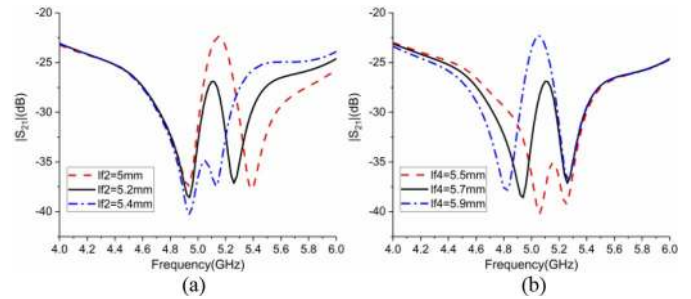

FIGURE 12. Simulated transmission characteristics of the proposed antenna for different parameters. (a) lf2 and (b) lf4.
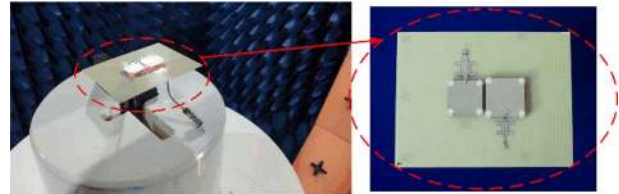

FIGURE 13. Prototype of the proposed patch antenna.

Fig. 12 shows the simulated transmission characteristic curves of the proposed antennas for these two parameters. When one parameter of the proposed filtering structures is analyzed, the other parameters are kept unchanged as listed in Table 1. It can be observed that the higher frequency transmission zero moves to the lower frequency band as *lf2* increases. Correspondingly, when *lf4* increases, the lower frequency transmission zero moves to the lower frequency band. Finally, the parameters *lf2* and *lf4* are chosen to be 5.2 mm and 5.7 mm in this work for the best decoupling performance.

III. MEASUREMENT RESULTS AND DISCUSSION

As shown in Fig. 13, the proposed compact patch antennas are fabricated and tested to verify the theoretical design. The S-parameters (reflection and transmission coefficients) are measured by vector network analyzer (VNA) and the measured results are shown in Fig. 14. The measured results are slightly different from the simulated ones due to the fabrication processing error and measurement error, but still meet the performance requirements. It shows the proposed filtering structures have a significant effect on the mutual coupling suppression. The isolation is more than 25 dB in both adjacent operating frequency bands when both the LB and HB antennas are well matched. Moreover, the measured results show that the isolation can reach to 30.3 dB at 4.9 GHz and 39.8 dB at 5.25 GHz.

Simultaneously, as shown in Fig. 13, radiation performance is measured by the TEM Radio 24 probe near-field measurement system. Fig. 15 demonstrates the simulated and measured radiation patterns of the proposed compact patch antennas at 4.9 GHz and 5.25 GHz. In the process of testing, when LB antenna is excited, the port of HB antenna is connected to a matching load and vice versa.
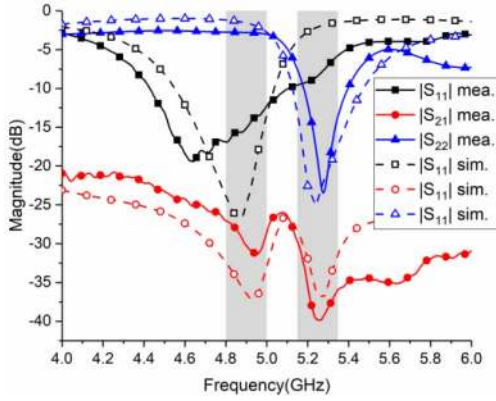
FIGURE 14. Simulated and measured S-parameters of the proposed compact patch antenna.
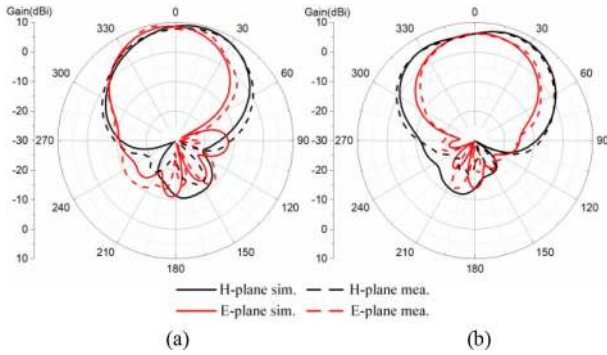

FIGURE 15. Simulated and measured radiation patterns of the proposed compact patch antenna at (a) 4.9 GHz and (b) 5.25 GHz.
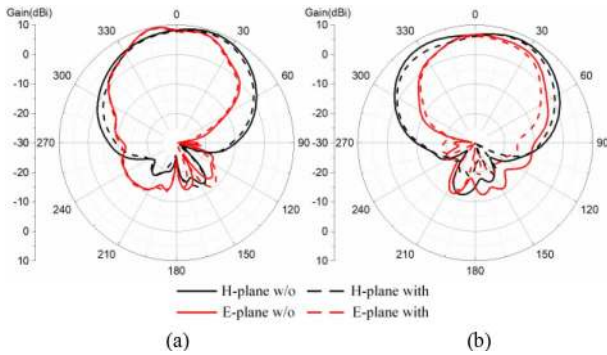

FIGURE 16. Measured radiation patterns of the antennas with and without the filtering structures at (a) 4.9 GHz and (b) 5.25 GHz.

It can be seen that the measured radiation pattern maintains a good agreement with the simulated one. In addition, the measured gain at the boresight direction reaches 7.8 dBi at 4.9 GHz and 6.2 dBi at 5.25 GHz. The measured radiation patterns of the antennas with and without filtering structures at 4.9 GHz and 5.25 GHz are plotted in Fig. 16. It can be seen that the radiation pattern of the antenna with the filtering structure is the same as the antenna without it. The radiation pattern is not affected by loading the filtering structure.

TABLE 2. Comparison of the proposed antenna and reference antennas.

Ref.	Method	Frequencies (GHz)	Edge to Edge spacing	Isolation Improvement (LB/HB)(dB)
[5]	Coupled Resonator	2.4/2.5	N/A	18/N/A
[20]	MADS and HDGS	3.7/4.1	$0.034\lambda_L$	17.7/18.1
[21]	Decoupling Network	6.4/8.2	/	24/6
[22]	Filtering Structure	1.8/2.05	$0.27\lambda_L$	20/10
[24]	FSS	0.8/4.2	$0.064\lambda_L$	N/A
Pro.	Open-loop Resonator	4.9/5.25	$0.016\lambda_L$	15/25

Note: λ_L represents the free-space wavelength at low resonant frequency.

A comparison of the proposed antennas with other reported antennas is presented in Table 2, one can be observed from which that the proposed antennas have two bands operating close to each other (the center frequency of the HB is only 1.07 times of the LB). It can also be seen that the proposed antennas achieve the smallest edge-to-edge spacing compared to other works. Moreover, the decoupling method reported in this work also has certain advantages in the improvement of the port isolation in both of the two resonant bands.

IV. CONCLUSION

This paper reports two patch antennas loaded with filtering structures are placed in a compact space and operating in adjacent frequency bands. The proposed filtering structures are composed of two open-loop resonators loaded at both sides of the feed-line. After a theoretical analysis of the proposed antennas, they have been fabricated and measured for design verification. The simulated and measured results prove that after loading the filtering structures, the port isolation can reach more than 25 dB in both operating bands for $|S_{11}| < -10$ dB in LB and $|S_{22}| < -10$ dB in HB, showing 15 dB and 25 dB isolation improvements at low and high resonant frequencies, respectively. Moreover, the decoupling frequency band can be controlled easily to meet different frequency requirements by adjusting the length of the filtering branch. In addition, the measured gain of the proposed antenna is up to 7.8 dBi at 4.9 GHz and 6.2 dBi at 5.25 GHz. The proposed filtering structure can effectively suppress the mutual coupling of antennas without deteriorating the other performance of the antenna, which provides an attractive function for solving mutual coupling problems of antennas operating in adjacent frequency bands.

REFERENCES

[1] *Making 5G NR a Commercial Reality*, Qualcomm Tech. San Diego, CA, USA, 2020. [Online] Available: https://www.qualcomm.com/media/documents/files/making-5g-nr-a-commercial-reality.pdf

[2] E. Khorov, A. Kiryanov, A. Lyakhov, and G. Bianchi, "A tutorial on IEEE 802.11ax high efficiency WLANs," *IEEE Commun. Surveys Tuts.*, vol. 21, no. 1, pp. 197–216, 1st Quart., 2019.

[3] "Study on signalling and procedure for interference avoidance for in-device coexistence, V11.2.0," 3GPP, Sophia Antipolis, France, Rep. TR 36.816, 2011.

[4] Z. Hu, R. Susitaival, Z. Chen, I.-K. Fu, P. Dayal, and S. K. Baghel, "Interference avoidance for in-device coexistence in 3GPP LTE-advanced: Challenges and solutions," *IEEE Commun. Mag.*, vol. 50, no. 11, pp. 60–67, Nov. 2012.

[5] L. Zhao, F. Liu, X. Shen, G. Jing, Y.-M. Cai, and Y. Li, "A high-pass antenna interference cancellation chip for mutual coupling reduction of antennas in contiguous frequency bands," *IEEE Access*, vol. 6, pp. 38097–38105, 2018.

[6] F. Yang and Y. Rahmat-Samii, "Microstrip antennas integrated with electromagnetic band-gap EBG structures: A low mutual coupling design for array applications," *IEEE Trans. Antennas Propag.*, vol. 51, no. 10, pp. 2936–2946, Oct. 2003.

[7] L. K. Yeung and Y. E. Wang, "Mode-based beamforming arrays for miniaturized platforms," *IEEE Trans. Microw. Theory Tech.*, vol. 57, no. 1, pp. 45–52, Jan. 2009.

[8] C.-Y. Chiu, C.-H. Cheng, R. D. Murch, and C. R. Rowell, "Reduction of mutual coupling between closely-packed antenna element," *IEEE Trans. Antennas Propag.*, vol. 55, no. 6, pp. 1732–1738, Jun. 2007.

[9] L. Zhao, L. K. Yeung, and K.-L. Wu, "A coupled resonator decoupling network for two-element compact antenna arrays in mobile terminals," *IEEE Trans. Antennas Propag.*, vol. 62, no. 5, pp. 2767–2776, May 2014.

[10] G. H. Zhai, Z. N. Chen, and X. M. Qing, "Enhanced isolation of a closely spaced four-element MIMO antenna system using meta-material mushroom," *IEEE Trans. Antennas Propag.*, vol. 63, no. 8, pp. 3362–3370, Aug. 2015.

[11] J. Guo, F. Liu, L. Zhao, Y. Yin, G. Huang, and Y. Li, "Meta-surface antenna array decoupling designs for two linear polarized antennas coupled in H-plane and E-plane," *IEEE Access*, vol. 7, pp. 100442–100452, 2019.

[12] X. Shen, Y. Liu, L. Zhao, G.-L. Huang, X. Shi, and Q. Huang, "A Miniaturized Microstrip Antenna Array at 5G Millimeter-Wave Band," *IEEE Antennas Wireless Propag. Lett.*, vol. 18, pp. 1671–1675, 2019.

[13] S.-W. Su, C.-T. Lee, and F.-S. Chang, "Printed MIMO-antenna system using neutralization-line technique for wireless USB-dongle applications," *IEEE Trans. Antennas Propag.*, vol. 60, no. 2, pp. 456–463, Feb. 2012.

[14] S. M. Amjadi and K. Sarabandi, "Mutual coupling mitigation in broadband multiple-antenna communication systems using feedforward technique," *IEEE Trans. Antennas Propag.*, vol. 64, no. 5, pp. 1642–1652, May 2016.

[15] S. Zhang and G. F. Pedersen, "Mutual coupling reduction for UWB MIMO antennas with a wideband neutralization line," *IEEE Antennas Wireless Propag. Lett.*, vol. 15, pp. 166–169, 2016.

[16] M. Li, L. Jiang, and K. L. Yeung, "Novel and efficient parasitic decoupling network for closely coupled antennas," *IEEE Trans. Antennas Propag.*, vol. 67, no. 6, pp. 3574–3585, Jun. 2019.

[17] M. Li, B. G. Zhong, and S. W. Cheung, "Isolation enhancement for MIMO patch antennas using near-field resonators as coupling-mode transducers," *IEEE Trans. Antennas Propag.*, vol. 67, no. 2, pp. 755–764, Feb. 2019.

[18] H.-L. Peng, R. Tao, W.-Y. Yin, and J.-F. Mao, "A novel compact dual-band antenna array with high isolations realized using the neutralization technique," *IEEE Trans. Antennas Propag.*, vol. 61, no. 4, pp. 1956–1962, Apr. 2013.

[19] X. Tan, W. Wang, Y. Wu, Y. Liu, and A. A. Kishk, "Enhancing isolation in dual-band meander-line multiple antenna by employing split EBG structure," *IEEE Trans. Antennas Propag.*, vol. 67, no. 4, pp. 2769–2774, Apr. 2019.

[20] F. Liu, J. Guo, L. Zhao, G.-L. Huang, Y. Li, and Y. Yin, "Dual-band metasurface-based decoupling method for two closely packed dual-band antennas," *IEEE Trans. Antennas Propag.*, vol. 68, no. 1, pp. 552–557, Jan. 2020.

[21] L. Zhao and K.-L. Wu, "A dual-band coupled resonator decoupling network for two coupled antennas," *IEEE Trans. Antennas Propag.*, vol. 63, no. 7, pp. 2843–2850, Jul. 2015.

[22] Z. Niu, H. Zhang, Q. Chen, and T. Zhong, "Isolation enhancement in closely coupled dual-band MIMO patch antennas," *IEEE Antennas Wireless Propag. Lett.*, vol. 18, pp. 1686–1690, 2019.

[23] B. C. Pan and T. J. Cui, "Broadband decoupling network for dual-band microstrip patch antennas," *IEEE Trans. Antennas Propag.*, vol. 65, no. 10, pp. 5595–5598, Oct. 2017.

[24] Y. Zhang, X. Y. Zhang, L.-H. Ye, and Y.-M. Pan, "Dual-band base station array using filtering antenna elements for mutual coupling suppression," *IEEE Trans. Antennas Propag.*, vol. 64, no. 8, pp. 3423–3430, Aug. 2016.

[25] H.-H. Sun, C. Ding, H. Zhu, B. Jones, and Y. J. Guo, "Suppression of cross-band scattering in multiband antenna arrays," *IEEE Trans. Antennas Propag.*, vol. 67, no. 4, pp. 2379–2389, Apr. 2019.

[26] Y. Zhu, Y. Chen, and S. Yang, "Decoupling and low-profile design of dual-band dual-polarized base-station antennas using frequency selective surface," *IEEE Trans. Antennas Propag.*, vol. 67, no. 8, pp. 5272–5281, Aug. 2019.

[27] D. Ahn, J.-S. Park, C.-S. Kim, J. Kim, Y. Qian, and T. Itoh, "A design of the low-pass filter using the novel microstrip defected ground structure," *IEEE Trans. Microw. Theory Techn.*, vol. 49, no. 1, pp. 86–93, Jan. 2001.

JIAYIN GUO (Graduate Student Member, IEEE) received the B.S. degree in electronic information engineering and the master's degree from Xidian University, Xi'an, China, in 2016 and 2018, respectively, where she is currently pursuing the Ph.D. degree in electromagnetic wave and microwave technology.

FENG LIU (Graduate Student Member, IEEE) received the B.S. degree in electronic information engineering from Xidian University, Xi'an, China, in 2016, where he is currently pursuing the Ph.D. degree in electromagnetic wave and microwave technology.

LUYU ZHAO (Senior Member, IEEE) was born in Xi'an, China, in 1984. He received the B.Eng. degree from Xidian University, Xi'an, in 2007, and the Ph.D. degree from the Chinese University of Hong Kong, Hong Kong, in 2014.

He has been an Associate Professor with the National Key Laboratory of Antennas and Microwave Technology, Xidian University, since 2016. From 2007 to 2009, he was a Research Assistant with the Key Laboratory of Antennas and Microwave Technology, Xidian University, where he was involved with software and hardware implementation of RF identification technologies. From 2014 to 2015, he was a Postdoctoral Fellow with the Chinese University of Hong Kong. From October 2015 to October 2016, he was a co-founder and CTO with Wyzdom Wireless Company Ltd. His current research interests include design and application of multiple antenna systems for next-generation mobile communication systems, innovative passive RF and microwave components and systems, millimeter wave and terahertz antenna array, and meta-material-based or inspired antenna arrays.

Dr. Zhao was a recipient of the Best Student Paper Award at 2013 IEEE 14th HK AP/MTT Postgraduate Conference and the Honorable Mention Award of the 2017 Asia–Pacific Conference on Antenna and Propagation. He is currently serving as an Associate Editor for IEEE ACCESS.

GUAN-LONG HUANG (Senior Member, IEEE) received the B.E. degree in electronic information engineering from the Harbin Institute of Technology, Harbin, China, and the Ph.D. degree in electrical and computer engineering from the National University of Singapore, Singapore.

He was with the Temasek Laboratories, National University of Singapore as a Research Scientist, and the Nokia Solutions and Networks System Technology as a Senior Antenna Specialist from 2011 to 2017. He is currently an Assistant Professor with the College of Information Engineering, Shenzhen University, Shenzhen, China. He also serves as the Deputy Director for the Guangdong Provincial Mobile Terminal Microwave and Millimeter-Wave Antenna Engineering Research Center. He has authored or coauthored more than 100 papers in journals and conferences. His research interests include design and implementation of planar antenna arrays, 5G base station and mobile RF front-end devices/antennas, phased antenna arrays, channel coding for massive MIMO applications, and 3-D printing technology in microwave applications. He is currently serving as an Associate Editor for IEEE ACCESS.

YINGSONG LI (Senior Member, IEEE) received the B.S. degree in electrical and information engineering and the M.S. degree in electromagnetic field and microwave technology from Harbin Engineering University, China, in 2006 and 2011, respectively, and the Ph.D. degree from both the Kochi University of Technology (KUT), Japan, and Harbin Engineering University in 2014. He was a Visiting Scholar with the University of California at Davis from March 2016 to March 2017. Since July 2014 he is a Full Professor with Harbin Engineering University. He is also a Visiting Professor with Far Eastern Federal University and KUT. His recent research interests are mainly in underwater communications, signal processing, compressed sensing, antenna, and antenna arrays. He is an Associate Editor of IEEE ACCESS and an Area Editor of the *AEÜ—International Journal of Electronics and Communications*. He also serves as a reviewer for more than 20 journals. He is a Senior Member of the Chinese Institute of Electronics.

YINGZENG YIN (Member, IEEE) received the B.S., M.S., and Ph.D. degrees in electromagnetic wave and microwave technology from Xidian University, Xi'an, China, in 1987, 1990, and 2002, respectively. From 1990 to 1992, he was a Research Assistant and an Instructor with the Institute of Antennas and Electromagnetic Scattering, Xidian University, where he was an Associate Professor with the Department of Electromagnetic Engineering from 1992 to 1996, and has been a Professor since 2004. His current research interests include the design of microstrip antennas, feeds for parabolic reflectors, artificial magnetic conductors, phased array antennas, and computer-aided design for antennas.